



This is a repository copy of *Modelling the potential for multi-location in-sewer heat recovery at a city scale under different seasonal scenarios*.

White Rose Research Online URL for this paper:
<http://eprints.whiterose.ac.uk/136415/>

Version: Accepted Version

Article:

Abdel-Aal, M. orcid.org/0000-0002-6726-5826, Schellart, A., Kroll, S. et al. (2 more authors) (2018) Modelling the potential for multi-location in-sewer heat recovery at a city scale under different seasonal scenarios. *Water Research*, 145. pp. 618-630. ISSN 0043-1354

<https://doi.org/10.1016/j.watres.2018.08.073>

Article available under the terms of the CC-BY-NC-ND licence
(<https://creativecommons.org/licenses/by-nc-nd/4.0/>).

Reuse

This article is distributed under the terms of the Creative Commons Attribution-NonCommercial-NoDerivs (CC BY-NC-ND) licence. This licence only allows you to download this work and share it with others as long as you credit the authors, but you can't change the article in any way or use it commercially. More information and the full terms of the licence here: <https://creativecommons.org/licenses/>

Takedown

If you consider content in White Rose Research Online to be in breach of UK law, please notify us by emailing eprints@whiterose.ac.uk including the URL of the record and the reason for the withdrawal request.

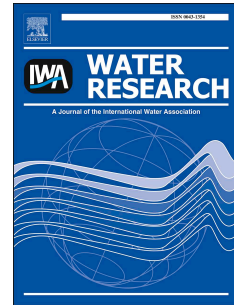


eprints@whiterose.ac.uk
<https://eprints.whiterose.ac.uk/>

Accepted Manuscript

Modelling the potential for multi-location in-sewer heat recovery at a city scale under different seasonal scenarios

Mohamad Abdel-Aal, Alma Schellart, Stefan Kroll, Mostafa Mohamed, Simon Tait



PII: S0043-1354(18)30703-6

DOI: [10.1016/j.watres.2018.08.073](https://doi.org/10.1016/j.watres.2018.08.073)

Reference: WR 14049

To appear in: *Water Research*

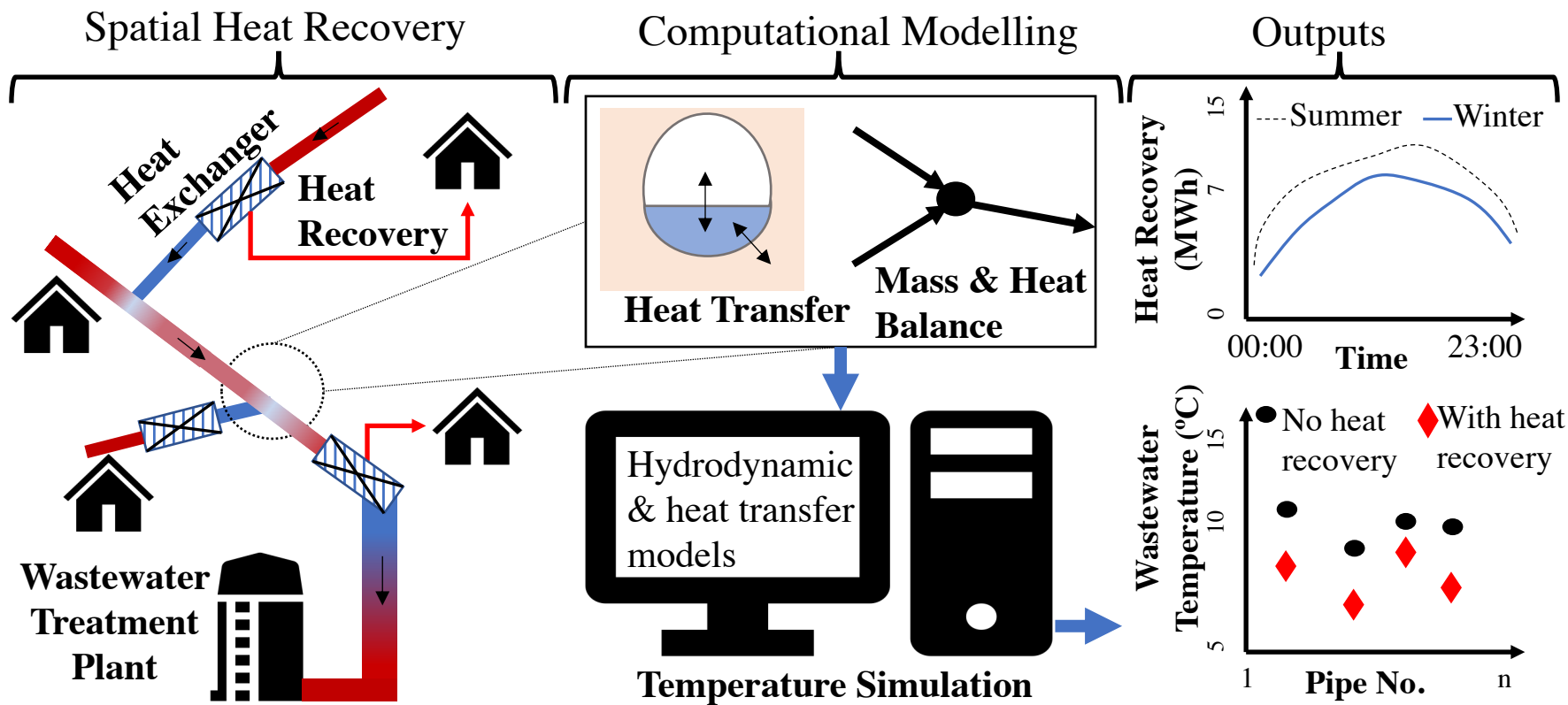
Received Date: 2 March 2018

Revised Date: 27 August 2018

Accepted Date: 31 August 2018

Please cite this article as: Abdel-Aal, M., Schellart, A., Kroll, S., Mohamed, M., Tait, S., Modelling the potential for multi-location in-sewer heat recovery at a city scale under different seasonal scenarios, *Water Research* (2018), doi: 10.1016/j.watres.2018.08.073.

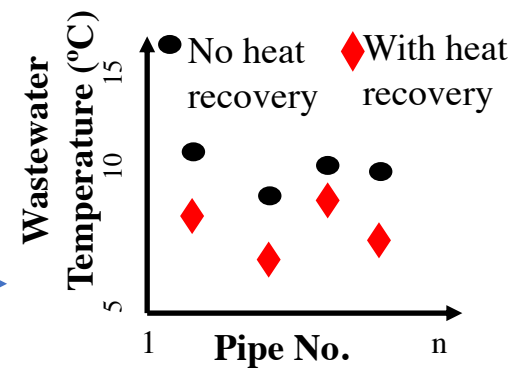
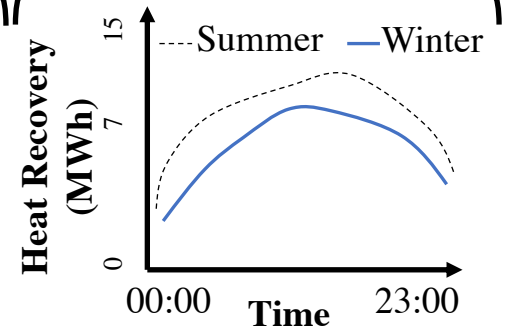
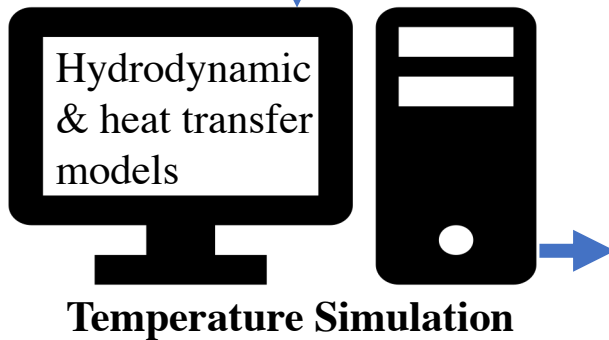
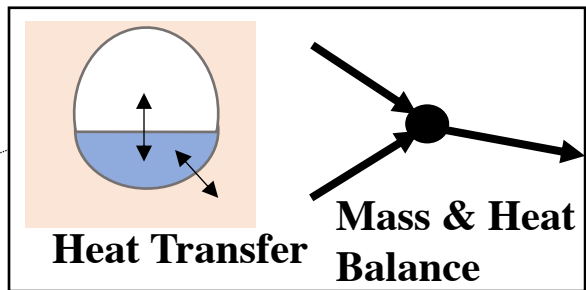
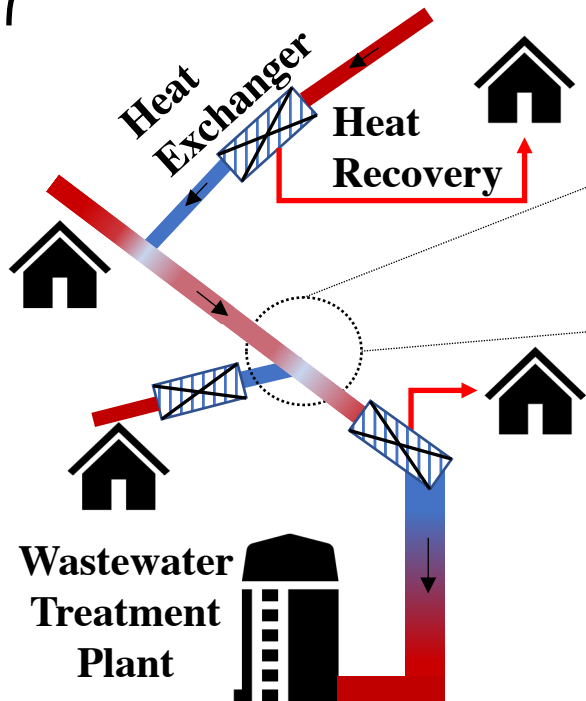
This is a PDF file of an unedited manuscript that has been accepted for publication. As a service to our customers we are providing this early version of the manuscript. The manuscript will undergo copyediting, typesetting, and review of the resulting proof before it is published in its final form. Please note that during the production process errors may be discovered which could affect the content, and all legal disclaimers that apply to the journal pertain.



Spatial Heat Recovery

Computational Modelling

Outputs



4
5 ¹ Pennine Water Group, Department of Civil and Structural Engineering, University of Sheffield, Mappin
6 Street, Sheffield, S1 3JD, UK.

7 ² Aquafin NV, Dijkstraat 8, 2630 Aartselaar, Belgium

8 ³ School of Engineering, University of Bradford, Bradford, BD7 1PD UK

9
10 *Corresponding author's email: m.abdel-aal@sheffield.ac.uk

11 **Abstract**

12 A computational network heat transfer model was utilised to model the potential of heat energy recovery at
13 multiple locations from a city scale combined sewer network. The uniqueness of this network model lies in
14 its whole system validation and implementation for seasonal scenarios in a large sewer network. The
15 network model was developed, on the basis of a previous single pipe heat transfer model, to make it suitable
16 for application in large sewer networks and its performance was validated in this study by predicting the
17 wastewater temperature variation in a sewer network. Since heat energy recovery in sewers may impact
18 negatively on wastewater treatment processes, the viability of large scale heat recovery across a network
19 was assessed by examining the distribution of the wastewater temperatures throughout the network and the
20 wastewater temperature at the wastewater treatment plant inlet. The network heat transfer model was applied
21 to a sewer network with around 3000 pipes and a population equivalent of 79500. Three scenarios; winter,
22 spring and summer were modelled to reflect seasonal variations. The model was run on an hourly basis
23 during dry weather. The modelling results indicated that potential heat energy recovery of around 116, 160
24 & 207 MWh/day may be obtained in January, March and May respectively, without causing wastewater
25 temperature either in the network or at the inlet of the wastewater treatment plant to reach a level that was
26 unacceptable to the water utility.

27
28 **Key words:** Heat recovery, heat transfer modelling, wastewater temperature prediction, clean thermal energy

29 **1 Introduction**

30 The potential heat available for recovery from sewers in the UK is thought to be significant, when estimated
31 theoretically, due to the high volumes of collected wastewater and the relatively high wastewater

32 temperatures found throughout the UK's combined and foul sewer networks. The UK's 347,000km of
33 sewers (Defra, 2002) are generally located in urban catchments where the domestic heat demand is
34 estimated to be around 300 TWh/year (ECUK, 2017). Considering heat recovery will result in a 2°C
35 wastewater temperature reduction (Buri & Kobel, 2005), the 11 billion litres of wastewater produced per day
36 (Defra, 2002), would potentially result in up to 390 TWh of heat recovery per year. This estimate is based
37 on the first law of thermodynamics, where the potential rate of heat recovery is the product of wastewater
38 mass flow rate, its specific thermal capacity and the consequent temperature reduction, and assumes a 100%
39 efficient heat recovery systems installed across all the UK's sewer networks.

40
41 The key technical challenge for efficient in-sewer heat recovery is to enable heat recovery sufficiently close
42 to points of local demand. To meet this challenge it is essential to quantify the impact of simultaneous heat
43 recovery at multiple locations within a sewer network. This "locality" constraint can reduce the overall
44 system potential. For example, in Austria, Kretschmer et al. (2015) estimated that 10% of Austrian houses
45 can benefit from heat recovered from wastewater. Another barrier for recovering heat from sewers is that
46 any reduction in wastewater temperature may cause difficulties with treatment processes and incur extra
47 costs at the end of system wastewater treatment plant (WwTP). It is therefore important to ensure that even
48 with multiple locations of heat recovery, the wastewater temperature reduction is limited at the inlet to the
49 WwTP. The nitrification process at the WwTP may be compromised by low wastewater temperatures, as
50 demonstrated by Shammas (1986), who tested the impact of varying the wastewater temperatures, from 4 to
51 35°C, on the nitrification quality and concluded that nitrification is much more effective at temperatures in
52 the upper part of this range, i.e. between 25 and 35°C. This finding is in line with a number of other studies
53 summarised in Metcalf & Eddy (2004), who reported that the optimum wastewater temperature for
54 nitrification was estimated to be between 25 and 35°C. Previous authors such as Wanner et al. (2005)
55 examined the impact of the reduction in temperature on wastewater nitrification and concluded that 1°C
56 reduction in wastewater temperature may reduce the nitrifier growth by 10%. Such a reduction would
57 require a 10% increase in the sludge retention time, to maintain the same nitrification quality achieved at the
58 unadjusted wastewater temperatures.

59
60 Previous studies have examined the variation in wastewater temperature in order to estimate the potential of
61 heat energy recovery and its impact on the treatment processes in WwTPs. Early work by Bischofsberger et
62 al. (1984) measured wastewater temperatures in Hamburg, Germany, for a year at five locations in a
63 combined sewer network, and observed that the wastewater temperatures varied between 7°C and 28°C
64 during the year. This temperature range was close to that observed in other in-sewer wastewater temperature
65 measurements reported in Dürrenmatt and Wanner (2008), Schilperoort and Clemens (2009), Cipolla and
66 Maglionico (2014), Abdel-Aal (2015) and Simperler (2015) in a number of combined sewer networks across
67 Europe.

68
69 Some studies have used simple relationships to estimate the impact of recovering heat energy on in-sewer
70 wastewater temperature, Kretschmer et al. (2016) estimated the potential heat energy recovery to be a linear
71 function of wastewater temperature, flow rate, temperature reduction and the heat capacity of water. No
72 estimate was made, by these authors, of the heat flux between the flowing wastewater and the in-sewer air
73 and the surrounding soil. Assessing the impact of heat energy recovery from a sewer pipe has led some
74 authors to develop more complex computational models to predict the wastewater temperature variation
75 along a sewer pipe taking into account heat flux into the surrounding soil and into the in-sewer air above the
76 wastewater flow. These models were developed for single pipes but by linking pipe sections they could be
77 used to estimate the cumulative effect along extended sewer pipes (Dürrenmatt, 2006; Dürrenmatt and
78 Wanner, 2008; Dürrenmatt and Wanner, 2014; Abdel-Aal et al., 2014; Abdel-Aal, 2015). The model
79 developed by Dürrenmatt and Wanner (2008), named TEMPEST, was the first capable of predicting
80 wastewater temperature in successive sewer pipes. Published studies have shown that TEMPEST was
81 implemented in a single string of sewer pipes; 1.85km long (Dürrenmatt and Wanner, 2014) and 3km long
82 (Sitzenfrei et al., 2017). The TEMPEST model was calibrated using a dataset collected over a 5 week period
83 from 14th February to 22nd March 2008. Elías-Maxil et al. (2017) developed a parsimonious model based on
84 TEMPEST yet excluded computation of the heat transfer between wastewater and in-sewer air. They
85 claimed that the heat flux between the wastewater and in-sewer air was not significant and could be ignored.

86 Elías-Maxil et al. (2017) used flow and temperature data collected in a 300 m long pipe to calibrate and
87 validate their model by adding hot water at a temperature of 50°C for six hours instead of simulating the
88 temperature variation of the wastewater. Abdel-Aal (2015) utilised measured flow and wastewater data
89 collected over a four month period in a small number of pipes within a combined sewer network to analyse
90 the sensitivity of the calibration parameters in the empirical equations describing the heat flux between the
91 in-sewer air and the wastewater and between the wastewater and surrounding soil. The calibration
92 parameters were varied from 10% to 400% of their default values, found in literature, and the impact of
93 these variations on the predicted downstream wastewater temperature was quantified. Increasing the heat
94 transfer coefficient between wastewater and in-sewer air by four times resulted in a 0.4°C variation, which
95 was the largest change among all other empirical heat transfer parameters taken into account, i.e. soil
96 thermal conductivity, soil penetration depth and pipe wall thermal conductivity. Hence, the sensitivity
97 analysis indicated that the heat flux between the wastewater and the in-sewer air should not be ignored if an
98 accurate estimate of the reduction in wastewater temperature along a sewer pipe is to be obtained.

99
100 The simulations reported in this paper utilised a network computational heat transfer model developed by
101 Abdel-Aal (2015), and validated in this work, which is able to predict in-pipe wastewater temperatures
102 throughout a large sewer network. The network heat flux model links an in-pipe heat transfer model,
103 accounting for air-wastewater, wastewater-pipe and wall-soil heat fluxes with a hydrodynamic sewer
104 network model. The model of Elías-Maxil (2015) was implemented on a single sub-catchment in a sewer
105 network and was used to predict in-pipe wastewater temperatures. It was not utilised to investigate the
106 impact of several locations of heat recovery on in-sewer wastewater temperatures. The uniqueness of this
107 work is the simultaneous modelling of heat recovery from multiple locations within a single network over
108 long durations. This has allowed the assessment of the in-sewer heat recovery reliability from a real large
109 sewer network over different periods within a year. Predicting the rate of heat recovery and assessing its
110 reliability are keys to making a believable economic assessment.

112 A heat transfer model was initially developed for a single sewer pipe and then modified and implemented in
113 a large sewer network, hence 'single pipe' and 'network' heat transfer models are used in this paper to
114 describe both model types respectively. This section briefly explains the method followed in the
115 development of the single pipe heat transfer model and how it was initially calibrated and validated. The
116 build-up, calibration and validation of the sewer network hydrodynamic model for the case study catchment
117 is then described. Following these descriptions an explanation is given as to how the single pipe heat
118 transfer model was further developed and then linked with the hydrodynamic sewer network model in order
119 to deliver a network heat transfer model. The predictive performance of the network heat transfer model was
120 then validated using collected field data from the case study catchment.

121
122 Calibration is defined in this paper as adjusting model parameters to minimise the differences between
123 predictions and observations . The validation process quantified model accuracy by implementing the
124 obtained calibrated parameters in model simulations and comparing predicted values with measured data
125 that were independent of those used for calibration. In the case of validating the hydrodynamic model, after
126 comparing measured and modelled flow rates and depths during dry weather flow days, head loss
127 parameters were adjusted to take into account the local energy losses and hence, improve the model
128 accuracy at specific locations. This section ends by explaining how the predicted wastewater temperatures,
129 in the network and at the WwTP inlet, were employed to model the potential heat energy recovery at
130 multiple locations on hourly basis, for different months.

131 2.1 The single pipe heat transfer model

132 This section briefly explains how a previously created single pipe heat transfer model was developed,
133 calibrated and validated so that it was then suitable for use in this study.

134 2.1.1 Development of the single pipe heat transfer model

135 The aim of this single pipe model was to produce an efficient sub-model that can be ultimately used in a
136 more complex model to obtain network temperature simulations while accounting for all the major heat
137 transfer processes observed within a single sewer pipe. Implementing the first law of thermodynamics and

accounting for the thermal convection between wastewater and in-sewer air and conduction between wastewater, at the invert level, and the surrounding soil through the pipe wall, the wastewater temperature variation along a single sewer pipe can be expressed by Equation 1, (Abdel-Aal, 2015).

$$T_{m+1} = T_m - \left(\frac{\frac{1}{R_{wa}}(T_m - T_{air}) + \frac{1}{R_{ws}}(T_m - T_{soil})}{\rho \times Q \times c_p} \Delta x \right) \quad (1)$$

When heat was recovered upstream of a sewer pipe in the network, it was assumed that wastewater temperature at the point downstream of any heat energy recovery location is reduced as a result of the heat recovery process, which can be estimated using Equation 2.

$$T_{m+1} = T_m - \left(\frac{HR}{\rho Q c_p} \right) \quad (2)$$

T is temperature (K), *m* is an expression of the wastewater temperature location within a longitudinal computational mesh along the pipe length, *R* is thermal resistivity (m.K/W) between wastewater and in-sewer air (wa) and between wastewater and soil (ws), Δx is the computational increment length stream-wise (m) based on dividing each pipe into 10 increments, ρ_w is the wastewater density (kg/m³), *Q* is the wastewater volumetric flow rate (m³/s) and *c_p* is the specific heat capacity for wastewater (J/kg.K), *HR* is the rate of heat recovered in Watts.

Equation 1 interprets the energy balance by expressing the thermal convection and conduction in terms of thermal resistivity which is a function of the wastewater velocity, its surface width and the pipe wetted perimeter which were ultimately computed using hydraulic data and pipe shapes retrieved from the sewer network hydrodynamic model.

The wastewater temperature was modelled with the assumption that the in-sewer pipe flow has a free surface. This is because typical DWF, in a sewer pipe, has a larger proportion of in-sewer air volume to that of wastewater. For example, the average measured wastewater depth to pipe diameter ratio was 8% in urban residential sewers and 42% in large sewer collectors (Abdel-Aal, 2015).

Edwini-Bonsu and Steffler (2006) installed a scrubber in a sewer pipe within a small network with 15 manholes to measure the influence of forced ventilation on the in-sewer air velocity by switching the scrubber on and off. Measured field data in the latter study showed that there was around a 10% variation in the in-sewer air velocity between trapped in-sewer air and forced ventilation conditions. Therefore, the

167 effect of active air ventilation in the sewer pipes was neglected in the in-sewer air/wastewater convection
168 based heat transfer model. The use of a conduction based heat transfer relationship between wastewater and
169 the surrounding soil is based on the assumption that there is no slip conditions between wastewater and inner
170 surface of the pipe wall, as detailed in Abdel-Aal (2015).

171 172 2.1.2 Calibration of the single pipe heat transfer model

173 The calibration of the single pipe heat transfer model was performed using data collected in four pipes of the
174 case study catchment. Hydraulic data was logged every 2 minutes, and soil temperature was measured every
175 20 minutes, while the upstream and downstream wastewater and in-sewer air temperatures were recorded
176 every 15 minutes in two larger collector sewers, and every 20 minutes in two smaller urban sewers. Such
177 data monitoring frequencies were found reasonable and adequate to calibrate and validate the single pipe
178 heat transfer model. The measured hydraulic and temperature data was logged continuously in February,
179 March and May 2012 for sewer pipes located in the case study catchment. Wastewater temperatures were
180 observed, by Tinytag (PBRF-5006-5m) sensors with $\pm 0.06^\circ\text{C}$ accuracy and better than 0.05°C resolution.

181
182 The importance of simulating the heat transfer between wastewater and in-sewer air for the prediction of
183 wastewater temperature variation, as mentioned above, led the authors to study and analyse the heat transfer
184 process between wastewater and in-sewer air. This relation was represented in Equation 1 by the thermal
185 resistivity between wastewater and in-sewer air (R_{wa}) and can be described by Equation 3.

$$186 \quad R_{wa} = \frac{1}{h_{wa} \times b} \quad (3)$$

187 *h_{wa} is the convective heat transfer coefficient between wastewater and in-sewer air ($\text{W}/\text{m}^2.\text{K}$), b is the*
188 *surface width of wastewater running in a sewer pipe (m).*

189
190 The traditional approach in estimating the heat transfer coefficient between water and air is through the use
191 of an empirical relationship. Flinspach (1973) proposed a relation, which is a function of the relative
192 wastewater velocity to that of in-sewer air, to estimate the heat transfer coefficient between wastewater and
193 in-sewer air (h_{wa}). However, the origin and underlying assumptions of Flinspach's relation is not well
194 recorded and it performed inconsistently. Hence, and in an attempt to improve the modelling accuracy, a
195 new more physically based parameterisation was developed to incorporate the influence of the wastewater

196 surface velocity, as it is associated with in-sewer air velocity (Edwini-Bonsu and Steffler, 2006) and depth,
 197 to estimate h_{wa} , using the dimensionless Froude number.

198
 199 The soil penetration depth and soil thermal conductivity were also calibrated to estimate the thermal
 200 resistivity between wastewater and the surrounding soil (R_{ws}), which is given by Equation 4. This is
 201 because, in addition to the heat transfer between wastewater and in-sewer air, the single pipe heat transfer
 202 model was sensitive to the soil penetration depth and its thermal conductivity (Abdel-Aal, 2015). Moreover,
 203 measuring the soil thermophysical properties in the field was impractical and the relevant parameters had
 204 wide ranges in literature.

$$205 \quad R_{ws} = \frac{t_p}{k_p \times wet.p} + \frac{d_s}{k_s \times wet.p} \quad (4)$$

206 t_p is the pipe wall thickness (m), d_s is the soil penetration depth (m), k_p and k_s are the thermal conductivities
 207 for pipe wall material and soil respectively (W/m.K) and $wet.p$ is the pipe wetted perimeter (m).
 208

209 Dürrenmatt (2006) and Dürrenmatt and Wanner (2014) incorporated more parameters such as, Chemical
 210 Oxygen Demand (COD) and its degradation rate, in their TEMPEST model. However, variation of these
 211 parameters showed insignificant impacts (less than 0.2%) on the predicted wastewater temperature
 212 (Dürrenmatt, 2006). In order to develop a computationally efficient simulation for use in a large sewer
 213 network, the single pipe heat transfer model was developed using only relationships which were significant
 214 in terms of the predicted wastewater temperature. Calibration of the single pipe heat transfer model was
 215 achieved using optimisation tools in Matlab to minimise the root mean squared error (RMSE) for each
 216 month's dataset, using Equation 5. A time step of 2 minutes, at which hydraulic data was measured, was
 217 utilised for calibrating the single pipe heat transfer model.

$$218 \quad RMSE = \sqrt{\frac{\sum_{j=1}^N (T_{Mj} - T_{Pj})^2}{N}} \quad (5)$$

219 T is the wastewater temperature ($^{\circ}C$), M and P stand for measured and predicted respectively, N is the total
 220 number of time steps and j is data point number.
 221

222 The model error was also computed to assess the single pipe heat transfer model accuracy in terms of over
 223 and under prediction, which was the average predicted minus measured wastewater temperatures for a full
 224 month dataset.

2.1.3 Validation of the single pipe heat transfer model

ACCEPTED MANUSCRIPT

Validation was carried out using independent datasets from that utilised for calibrating the single pipe heat transfer model. The validation data was measured in sewer sites with similar characteristics to those used for calibration, i.e. large collector and urban sewers, and in the same period, using identical sensor types described in section 2.1.2. The model validation was assessed by the RMSE and modelling errors in a similar manner described in section 2.1.2.

2.2 The hydrodynamic sewer network model

Hydraulic data, such as the wastewater flow rate, velocity and depth is necessary for simulating the in-sewer wastewater temperatures. Therefore, a hydrodynamic model built in Infoworks CS, was used to provide the hydraulic data for the case study sewer network. The Infoworks CS model used a numerical scheme to solve the Saint-Venant and the Colebrook-White equations in order to calculate wastewater velocity and depth in all pipes throughout the network at all time steps.

The sewer network used in this study, consisted of 3093 links, 3048 of which were sewer pipes (conduits) while the rest of the links were valves, pumps and other connections. There were 2296 sub-catchments which can contribute two types of flow. Most catchments contributed 'foul' (domestic wastewater inflow), as well as 'trade' flows, which referred to industrial inflows and occurred in a limited number of the catchments. Some of the pipes carrying trade flows did not contain flow at all timesteps, and occasionally there were flow reversals in this network. Hence, both zero and negative values of flow were possible in the hydraulic output from this Infoworks CS model. Therefore, the hydraulic output data was filtered by replacing zero and negative values of wastewater depth, velocity and flow with a very small positive default values (0.0001 m, m/s or m³/s) to ensure the stability of the heat transfer modelling. This filtration process had an insignificant effect on the predicted total daily wastewater volume, the difference did not exceed 0.5% in January, March and May, while the adjustment of negative and zero wastewater level values accounted for less than 0.7% of the total values in the three months.

In this study only dry weather flow (DWF) conditions on working days was considered. The DWF days were selected by observing the flow variation plots in the measurement period for each site. The rainfall events were obvious, hence periods without rainfall that showed consistent flow patterns for a continuous period of three or more days were considered to be DWF days.

2.2.2 Building and calibration of the hydrodynamic model

Aquafin (2014) standards was utilised to construct the Infoworks CS model. The hydrodynamic model was built using historical datasets of the pipe geometries, characteristics and connectivity. This data was compared to records of the current state of the network and field observations and the model geometry was corrected when needed. The DWF at each model input node was estimated based on the local population equivalent (PE), the average wastewater production rate per person and an empirical diurnal wastewater profile. Trade flow was predicted from records of the maximum permitted industrial inputs. The diurnal variation in flow was calibrated using measured flow rates at seven locations across the network during two dry weather days.

2.2.3 Validation of the hydrodynamic model

A flow monitoring campaign was carried out specifically for this study that included the installation of flowmeters in seven locations across the sewer network. The modelled wastewater flow was visually compared with measured data based on time-series datasets and the total flow was checked against the measured downstream flow of the entire network. In cases where the observation showed large discrepancies (e.g. bias in wastewater depth greater than 2 cm), the model was updated by adjusting relevant parameters, such as the local and pipe head loss coefficients and the height of the fixed sediment layer, so that the modelled results better matched the observed data. An acceptable level of performance level was determined by an experienced hydrodynamic modeller through visual comparisons between modelled and monitored values of flow rates at the seven locations throughout the network.

2.3 The network heat transfer model

This model was created by developing and using the single pipe heat transfer model and linking this to the hydrodynamic model. The simulation of wastewater temperatures at all locations within a large sewer

277 network was achieved by implementing the network heat transfer model. This section explains how the
278 model was developed, used for identifying heat recovery locations and validated.

279 2.3.1 Development of the network heat transfer model

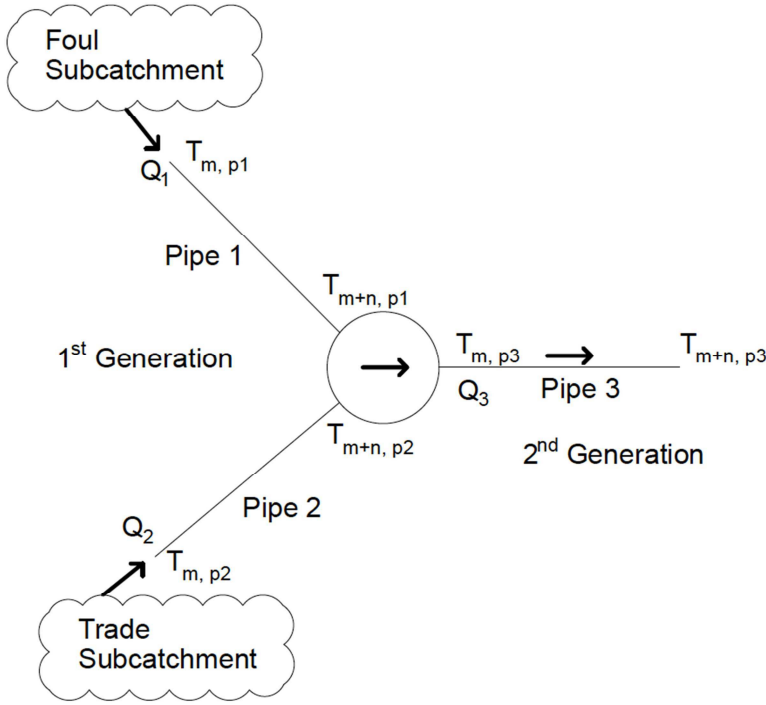
281 Three main datatypes were generated from the Infoworks CS model, these are: the details of the network
282 links, hydraulic data and soil types. The details of the network links provided information on the way the
283 links were connected, link type, geometry, dimension and the material of each link in the network. The link
284 types mainly included conduits (pipes), valves and pumps, and each link had a unique identifier number
285 which can be utilised to identify its streamwise location of the network. The hydraulic data consisted of the
286 Infoworks CS modelled wastewater flow rate, velocity and depth in each link for a full year at two minute
287 timesteps. Table 1 shows a summary of the data and pipe details retrieved from the hydrodynamic model
288 and literature, in order to create the network heat transfer network model.

Table 1: Summary of the data used to create the network heat transfer model.

Category	Model input	Value / Range	Unit	Notes
Sewer temperatures	In-sewer air temperature	8.6 to 15.5	°C	Measured in the case study sewers during January, March and May 2012.
Hydraulic data for each pipe	Wastewater flow rate	0.0001 to 10.6	m ³ /s	Full year Infoworks CS simulations, 2 minutes time step. Negative or zero values were replaced by 0.0001 m, m/s or m ³ /s. Assumed stream-wise flow direction.
	Wastewater velocity	0.0001 to 2	m/s	
	Wastewater depth	0.0001 to 4.3	m	
Sub-catchments connected to the sewer network	Flow of wastewater discharged from trade	0.0001 to 0.007	m ³ /s	Full year Infoworks CS data, 2 minutes time step.
	Flow of wastewater discharged from foul	0.0001 to 1.85	m ³ /s	
	Trade wastewater temperature	15	°C	Assumed, based on model validation and agrees with Schilperoort & Clemens (2009) measurements.
	Foul (residential) wastewater temperature	15	°C	
Specifications of each sewer pipe	Sewer pipe shapes	Circle, egg or rectangular		Hydrodynamic model
	Sewer pipe materials	Concrete, steel, reinforced concrete, clay, brick, or polyvinyl chloride.		
	Sewer length	1 to 801	m	
	increment length stream-wise (Δx), based on diving each pipe into 10 increments	0.1 to 8	m	
	Sewer diameter	0.08 to 5.25	m	
Sewer wall thickness	0.053 to 0.3	m		
Soil details	Soil type surrounding each pipe	Sand		Provided by the regional soil database.
	Soil temperature	9 & 10	°C	Measured in case study catchment.
Pipe linkages	Pipe identifiers	The unique pipe identifiers		Retrieved from the hydrodynamic model. The ids are used to organise the pipes in their stream-wise location and to connect incoming branches at the correct locations, and to connect the incoming foul, rainfall and trade flows in the right locations.
	Sub-catchment identifiers	The unique sub-catchment identifiers		

Equation 1 was used for each pipe in the network where the upstream temperature (T_m) can correspond to either a 1st generation or 2nd and higher generation pipes. The different pipe generations reflect the streamwise locations of the pipe within the sewer network. Pipes of the 1st generation transport wastewater from the most upstream area of the network, e.g. foul or trade sub-catchments, to the 2nd generation pipes and consequently to the 3rd, 4th and up to the 7th generation pipes before reaching the WwTP. Figure 1 illustrates how the pipes were connected in the network at different generations. The wastewater temperature for the 1st generation pipes was assumed to be equal to that discharged from the relevant sub-catchment,

315 while the upstream wastewater temperature for the 2nd and higher generations was assumed to be equal to
 316 that of the downstream temperature of the preceding generation. When more than one pipe was connected to
 317 one or more pipes, as shown by Figure 1, the upstream wastewater temperature was computed by Equations
 318 6 and 7.



320

321 *Figure 1: Example of two pipes connected to a third pipe in the sewer network. T_m and T_{m+n} are the pipe*
 322 *upstream and downstream wastewater temperatures respectively, n is the number of mesh points along the*
 323 *pipe length. p and T stand for pipe and wastewater temperature respectively. The flow is assumed to be*
 324 *heading into one direction shown by the arrows.*

325

$$326 \quad Q_3 = Q_1 + Q_2 \quad (6)$$

$$327 \quad T_{m,p3} = \frac{T_{m+n,p1} \times Q_1 + T_{m+n,p2} \times Q_2}{Q_3} \quad (7)$$

328 *where; T is temperature (K or °C) and p 1,2 & 3 refer to pipes 1, 2 & 3 respectively as illustrated in Figure*
 329 *1. m is the mesh location of the predicted wastewater temperature along the pipe length, n is the number of*
 330 *mesh points along the pipe length.*

331

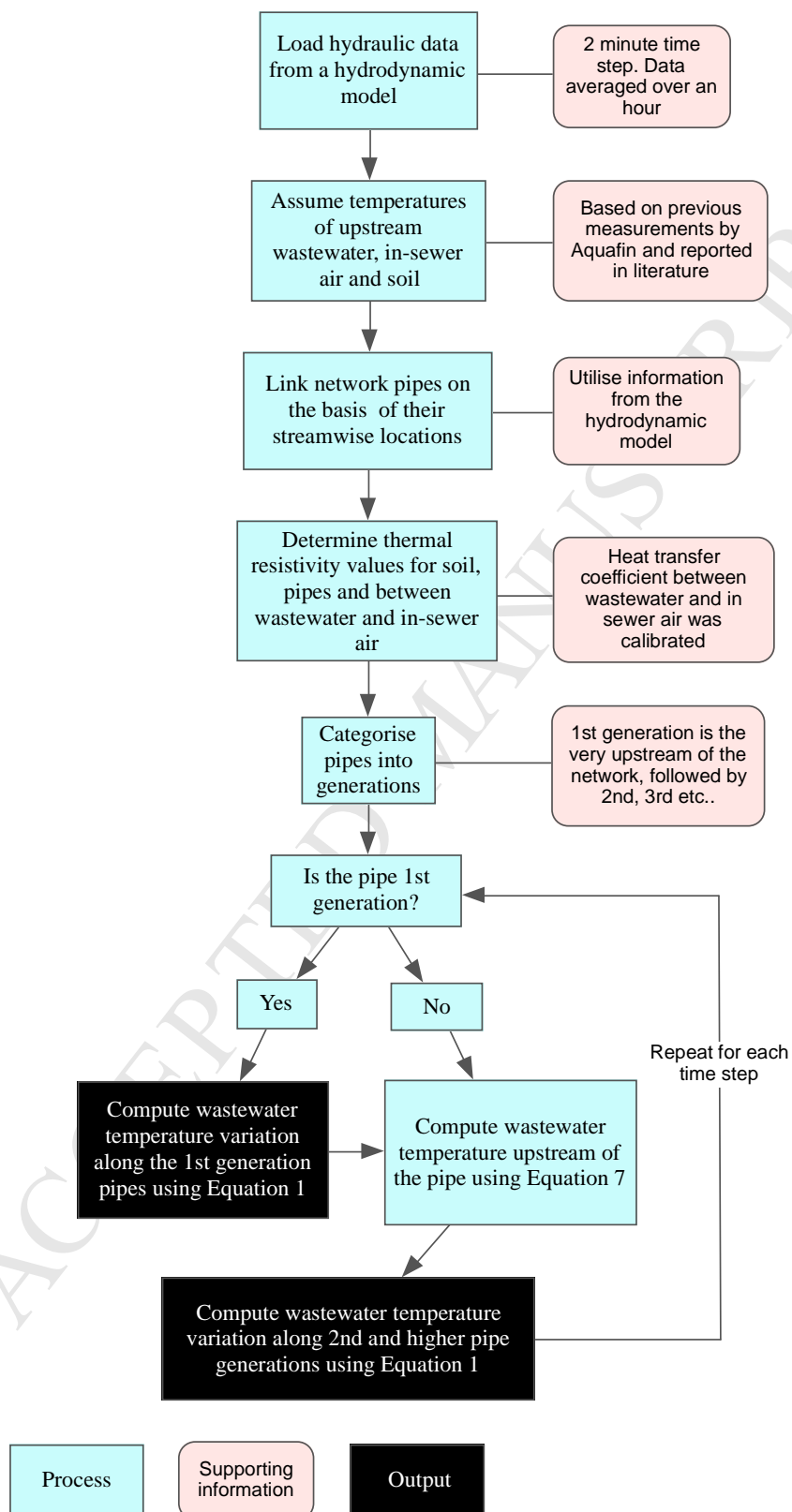
332 Model input temperatures, i.e. of wastewater at the 1st generation pipes, soil and in-sewer air, can be
 333 retrieved from literature based on field seasonal data (see Table 1). The model output is the wastewater
 334 temperature variation along the length of each sewer pipe in the network, and the WwTP influent
 335 temperature. This paper's results will focus on the minimum wastewater temperatures in the network and on

336 the WwTP influent to enable the assessment of the potential heat energy recovery from the sewer network.

ACCEPTED MANUSCRIPT

337 Figure 2 summarises the process followed for developing the network heat transfer model, which was used

338 in this paper.



339

340 Figure 2: Flowchart of the process followed for the network heat transfer model development.

2.3.2 Determination of heat recovery locations

ACCEPTED MANUSCRIPT

The heat energy recovery locations were determined by the network heat transfer model based on selection criteria for each sewer pipe determined by the model user, these are: defining a minimum wastewater temperature and a minimum flow rate. Section 2.5 explains the selection criteria used in this work to create the heat energy recovery scenarios.

2.3.3 Validation of the network heat transfer model

The network heat transfer model was validated using measured data in four different manhole locations within the case study 3000 pipe network. The same Tinytag sensors described in section 2.1.2 were used for the network model validation. Sewer pipes with different sizes and various streamwise locations were selected for validation to reflect the diverse pipe characteristics in a large sewer network. Locations 1 and 2 were 1st and 2nd generation sewer pipes respectively, while locations 3 and 4 were 3rd generation pipes, and distances between the four locations varied from 48 to 1600 meters. For effective data collection and sensor maintenance, the distances between monitored locations were relatively short to support Aquafin operators carry frequent site visits. Figure 3 shows the locations of the measured temperatures in the sewer pipes.



Figure 3: Locations of monitored sewer sites used to validate the network heat transfer model

357 Datasets used for validation were recorded on 16th January, 12th March and 5th May 2012. Hourly averages
358 of the measured data were obtained and used for validating the network heat transfer model in each of the
359 four locations. The network heat transfer model validation was based on the difference between measured
360 and predicted wastewater temperatures on an hourly basis. The RMSE for each day (N=24) was also
361 computed using Equation 5 to show the overall model daily performance. The network model error, defined
362 as the hourly average predicted minus measured wastewater temperatures, was computed to investigate the
363 model over and under prediction. A foul temperature of 15°C, which is within the range measured by
364 Schilperoort and Clemens (2009), was used for validating the network model. This is considered to be a
365 relatively low foul temperature, when compared with that measured by the aforementioned authors which
366 reached 35°C, and hence the validated model represents challenging input boundary conditions for heat
367 energy recovery applications.

368 369 2.4 Assessment of the heat energy recovery viability

370 The viability of heat energy recovery in this paper was assessed by predicting and examining the wastewater
371 temperature in the sewer network and at the WwTP influent. The influent WwTP temperature can affect the
372 nitrification quality as mentioned in Section 1, and the wastewater temperature in the sewer network needed
373 to be well above the freezing point. Water utilities may have different regulations regarding thresholds for
374 these temperatures. This paper measured the viability of heat energy recovery by referring to Aquafin's
375 requirements regarding wastewater temperatures. Aquafin (2015) considers minimum wastewater
376 temperatures of 5°C in the sewer network to be viable as long as the WwTP influent stays 9°C or above.
377 Therefore, the aforementioned temperatures were assumed to be the thresholds criteria for a viable heat
378 energy recovery option. These temperature thresholds can be varied by the model user to simulate the
379 potential of heat recovery within the limits provided by the local regulations.

380 2.5 Heat energy recovery scenarios

381 Three scenarios were considered in this study to reflect extreme cold (January), cool (March) and moderate
382 (May) weather conditions of the winter, spring and summer seasons. The three scenarios utilised hydraulic
383 data from Infoworks CS. Apart from the variation in the hydraulic data, the main differences between the

384 three scenarios were the measured in-sewer air and soil temperatures, which ranged between 8.6 and 15.5°C
385 and between 9 and 10°C respectively. The calibrated heat transfer parameters were utilised for modelling
386 each scenario. Table 3 lists the values of the heat transfer parameters used in each seasonal scenario.

387
388 The minimum wastewater flow criterion for a pipe to be qualified for a heat energy recovery location was
389 set to be 25, 50, 100 & 200 L/s. Although some practitioners recommend minimum flow range of 10 to 15
390 L/s (DWA, 2009), the 25 L/s value was found to be appropriate in such a large sewer network. This is
391 because the majority of the pipes in the sewer network would have a wastewater flow rate between 10 and
392 15 L/s during a DWF day, which would result in a very large number of heat recovery locations and
393 consequently, wastewater temperature reductions would be too large. The values of 25, 50, 100 and 200 L/s
394 were decided based on a number of trials. A minimum wastewater temperature for a pipe to be qualified for
395 heat recovery was decided to be 9°C, which was equal to the minimum required for the WwTP influent.
396 Table 2 describes the three scenarios and their relevant assumptions. A rate of 200 kW heat was assumed to
397 be recovered from locations that meet the temperature and flow conditions set as minimum criteria. This
398 assumption was based on a study performed by Vlario (2015) where estimates of the total conventional
399 radiator capacity for 93 flats in Belgium were in the order of 200 kW. The DWF days were found consistent
400 in terms of the wastewater flow variation, and hence, a random working day with DWF was selected in
401 January, March and May to show the potential heat energy recovery and its implications on wastewater
402 temperatures. Each of the three seasonal scenarios shows the potential of heat energy recovery during the
403 selected day (00:00 AM to 23:59 PM) on an hourly basis.

Table 2: Scenarios of heat energy recovery in January, March and May using different measured temperatures of in-sewer air. HR is the rate of heat recovery.

Scenario	Date in 2012	Time of HR on hourly basis hh:mm	HR from pipes with		HR kW/pipe	Temperatures			Network flow L/s
			Min. Flow L/s	Min. Temp °C		Foul	In-sewer air °C	Soil	
1	Monday 16 th January	00:00 to 23:59		9			8.6 to 9.3	9	
2	Monday 12 th March	00:00 to 23:59	25, 100 & 200	50, 9	200	15	9.7 to 10.8	9	0.1 to 340
3	Friday 4 th May	00:00 to 23:59		9			13.7 to 15.5	10	

Hours between 07:00 and 08:00 AM had the highest heat energy demand in each of the scenario days, based on smart meter readings for 100 residential homes across the UK (AECOM, 2014). Therefore, to investigate the potential of heat recovery during DWF and relatively high heat demand conditions in more details, data between 07:00 and 08:00 AM was utilised to present model outcomes using probability distribution function (PDF) plots of minimum wastewater temperatures in the network.

3 Results

This section shows the calibrated parameters of the single pipe heat transfer model. The section then presents the validation results for the single pipe and network heat transfer models. The potential of heat energy recovery, on an hourly basis, in each scenario and the implications of this in terms of wastewater temperature variation are described in the final part of the section. The results of modelling each scenario, between 7:00 and 8:00 AM, are presented in more details through PDF plots and a summary table.

3.1 Calibration results for the single pipe heat transfer model

Table 3 shows the values of calibrated parameters used in the single pipe heat transfer model, in urban and large collector sewers.

427 *Table 3: Values of calibrated parameters used in the single pipe heat transfer model. k_s and d_s are the soil*
 428 *thermal conductivity and its penetration depth respectively, h_{wa} is the heat transfer coefficient between*
 429 *wastewater and in-sewer air, R_{wa} and R_{ws} stand for thermal resistivity between wastewater and in-sewer air*
 430 *and soil respectively.*

Month	k_s/d_s (W/m ² .K)		h_{wa} (W/m ² .K)		R_{wa} (m.K/W)		R_{ws} (m.K/W)	
	Residential	Collector	Residential	Collector	Residential	Collector	Residential	Collector
February	No data	100	No data	66	No data	0.02	No data	0.07
March	67	100	32	58	0.07	0.02	0.32	0.08
May	63	100	7	50	0.28	0.03	0.31	0.08

431

432

433 The calibrated parameters showed different values for different months and site characteristics, particularly
 434 h_{wa} . This is likely to be due to the seasonal differences in the thermophysical properties of the in-sewer air
 435 and soil caused by the temperature variation which would influence their thermal conductivity. This effect
 436 was also described in Abdel-Aal (2015). Although groundwater level may influence the soil temperature,
 437 measured data showed soil temperatures in the case study catchment did only vary slightly, by 1 °C. This
 438 may be due to the existence of groundwater, which its level was not measured.

439 3.2 Validation results for the single pipe heat transfer model

440 The calibrated heat transfer coefficient between wastewater and in-sewer air improved the modelling
 441 accuracy, where the monthly RMSE obtained previously using the Flinspach (1973) relation was up to
 442 0.83°C (Abdel-Aal, 2015) while implementing the new parameterisation on the same sewer pipe using an
 443 identical validation method showed RMSE values of 0.13°C (February), 0.43°C (March) & 0.28°C (May).
 444 The monthly modelling errors in the validated model, for a single pipe, ranged between -0.17 and 0.09°C in
 445 winter and between -0.04 and 0.06°C in summer. The ranges of the modelling errors indicate over and under
 446 prediction in each sewer pipe, which minimise the overall error in the predicted wastewater temperatures
 447 across the network since the error is unlikely to accumulate. Based on the modelling errors, the resolution
 448 for temperature results is reported to the nearest one decimal place.

449

3.3 Validation results for the network heat transfer model

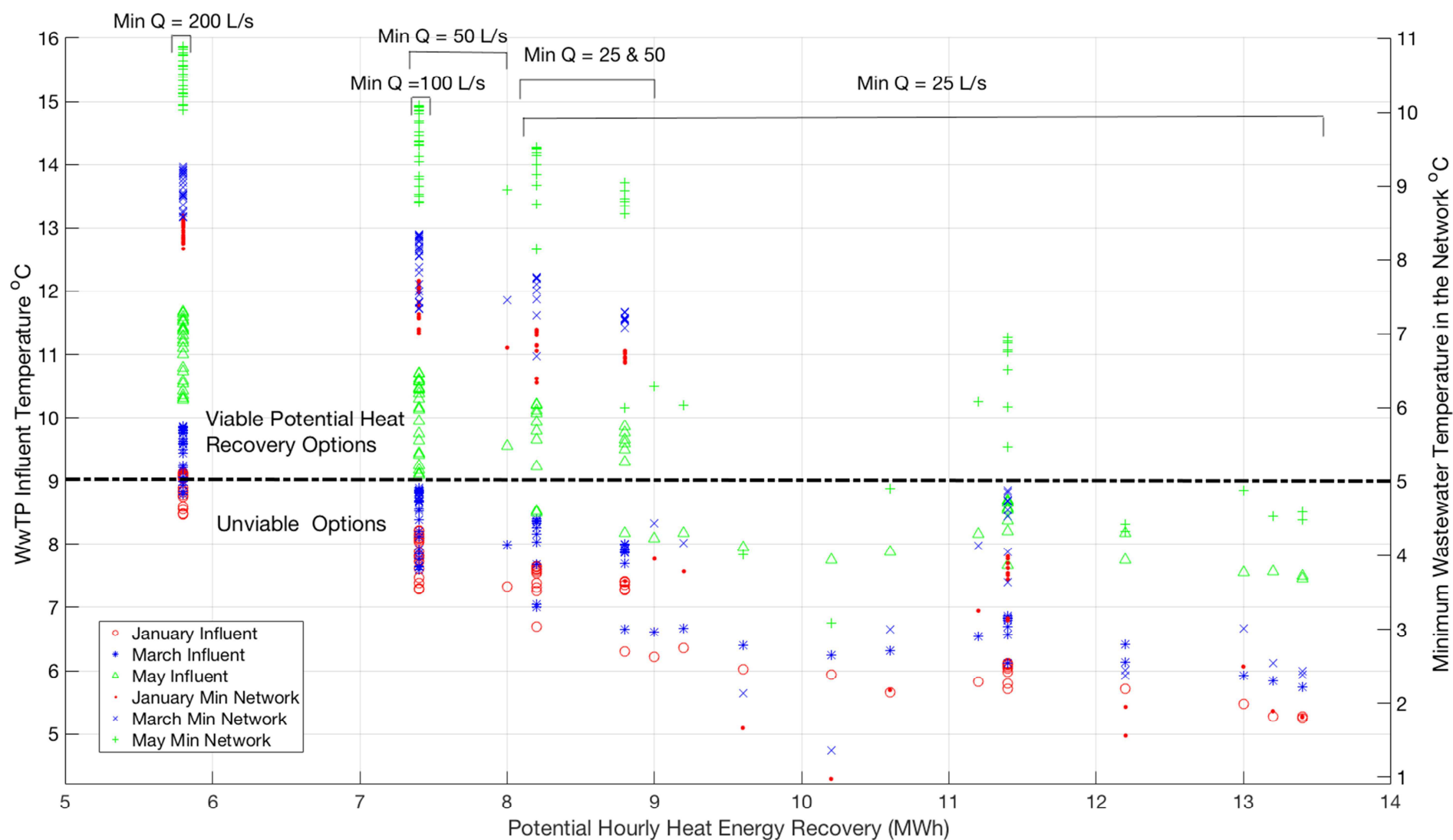
ACCEPTED MANUSCRIPT

Validation of the network heat transfer model resulted in daily RMSE values that varied from 0.44°C in May, 0.45°C in January to 0.72°C in March, which can be considered reasonable for the model purpose of assessing the potential of heat recovery from sewer networks. The relatively high RMSE in March is likely due to the larger temperature fluctuations in the day which varied by 4°C, compared to 2°C in January and May. The mechanism of heat transfer is affected by the seasonal temperature variation and hence, calibrating heat transfer parameter under such large temperature variation, in March, is expected to produce discrepancy in predicted results.

The hourly modelling errors varied between -0.60 to 0.87°C in January, -0.76 to 1.2°C in March and -1.2 to 0.90°C in May. Similar error implications to that found in the single pipe heat transfer model validation, the errors in predicted wastewater temperatures, across the network, is likely to be reduced since the model under and over predicts, shown by the negative and positive modelling errors respectively, in the three seasons.

3.4 Scenarios 1, 2 & 3, heat energy recovery between 00:00 & 23:59 PM

Figure 4 shows the potential of heat energy recovery on an hourly basis over a day in January, March and May, the minimum network temperatures and corresponding WwTP influent temperatures. The points plotted in Figure 4 reflect the network heat transfer model outcomes for 200 kW/pipe heat recovered from pipes with flow rates higher than 25, 50, 100 & 250 L/s, during 24 hour periods in January, March and May. The DWF variation along the day of each scenario was found to be consistent in each month. It was also noticed that DWF reached its minimum value during the hours between 03:00 AM and 04:00 AM and was almost constant otherwise.



475 *Figure 4: Potential heat energy recovery options, WwTP influent temperatures (left axis) and minimum wastewater temperatures in the network (right axis) in*
 476 *January, March and May, when 200 kW/pipe is recovered from pipes with flow rates higher than 25, 50, 100 & 200.*

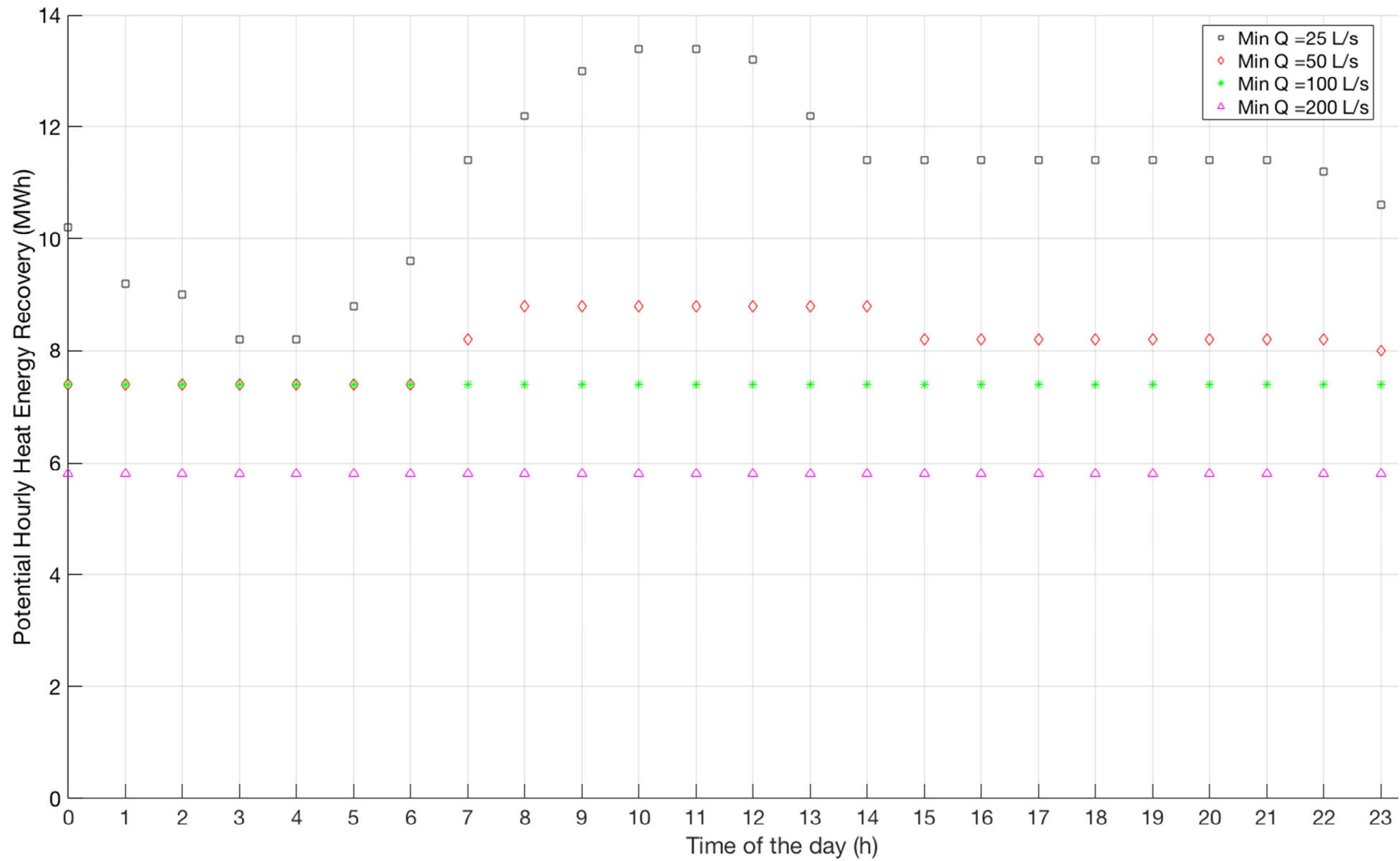
477 The maximum potential heat energy that can be recovered from the sewer network, over an hour, was 13.4
478 MWh for January, March and May. One can notice, from Figure 4, the impact of this 13.4 MWh recovery
479 on the WwTP influent temperature, which varied from 5.3°C (January), 5.7°C (March) to 7.5°C (May).
480 Higher values for the minimum required pipe flow (e.g. 200 L/s) to recover 200 kW/pipe presented lower
481 number of locations, which estimated less potential heat energy recovery. This is expected since 97% of the
482 sewer pipes in the network had flow rates less than 27 L/s. In this work, heat energy recovery is considered
483 viable only when the WwTP influent is above or equal to 9°C and minimum wastewater temperature in the
484 sewer network is 5 °C. Such viable options were presented by the 133 points (out of 288) plotted above the
485 dash dotted line in Figure 4. The network heat transfer model predicted 116, 160 & 207 MWh/day to be
486 recovered in January, March and May respectively. The latter predictions of heat energy recovery are the
487 total of maximum hourly values that were considered viable for each day.

488
489 The time of the day had a noticeable effect on the rate of heat recovery and minimum wastewater
490 temperatures in the network and at the WwTP influent due to the variation of the DWF along the day. In
491 January, viable heat recovery was predicted to be possible during the time periods from midnight to 01:00
492 AM, and between 06:00 AM and 23:00 PM, in March it was from midnight to 02:00 AM and between 05:00
493 AM and 23:00 PM, whilst in May viable heat recovery was possible in all the 24 hours period. Figure 5
494 shows the potential heat energy recovery on an hourly basis along the 24-hour periods in January, March
495 and May. The rate of potential heat recovery, at a particular time of the day, was the same in each month,
496 hence Figure 5 only shows the results of the January scenario. The relatively low flow rate between 03:00
497 and 04:00 AM resulted in a smaller number of locations (41), which was much lower than other cases, e.g.
498 67 potential locations were identified between 10:00 and 11:00 AM in the three scenarios for heat recovery
499 from pipes with minimum flow of 25 L/s. Therefore, the maximum heat recovered between 03:00 and 04:00
500 AM was 8.2 MWh which was less than that of 13.4 MWh predicted between 10:00 and 11:00 AM.
501 Nevertheless, the minimum WwTP influent temperature in January, between 03:00 and 04:00 AM, was
502 higher (8 °C) than that between 10:00 and 11:00 AM (7 °C), and similarly, the minimum network

503 temperature was always above 6°C between 3:00 and 04:00 AM, which was much higher than its 1.8°C
ACCEPTED MANUSCRIPT
504 equivalent obtained between 10:00 and 11:00 AM.

ACCEPTED MANUSCRIPT

505



506

507

Figure 5: Potential heat energy recovery on hourly basis in 16th January. Other months showed the same hourly heat energy recovery.

3.5 Scenarios 1, 2 & 3: heat energy recovery between 07:00 & 08:00 AM

ACCEPTED MANUSCRIPT

This section shows the PDF of minimum network temperatures for each scenario between 07:00 & 08:00 AM and summarises the outcomes of the modelled scenarios during the selected hour. The area under the curve between two temperature points, in a PDF plot, would indicate the probability of having pipes with temperature values corresponding to these points. The PDF was also plotted for the sewer network when there was no heat recovery; to enable the comparison with the heat recovery scenarios. For effective utilisation of the thermal energy content in the sewer network, an ideal scenario would show a shift towards the left, relative to the 'no heat recovery' PDF, while maintaining the network temperature thresholds.

3.5.1 Scenario 1, between 07:00 & 08:00 AM

Figure 6 shows the PDF of wastewater temperature at the downstream end of each pipe in Scenario 1 between 7:00 and 8:00 AM. Recovering heat in Scenario 1 would reduce the wastewater temperatures in the network, which was evidenced by Figure 6 showing higher probabilities of wastewater temperatures being between 10 and 12°C than that when no heat was recovered.

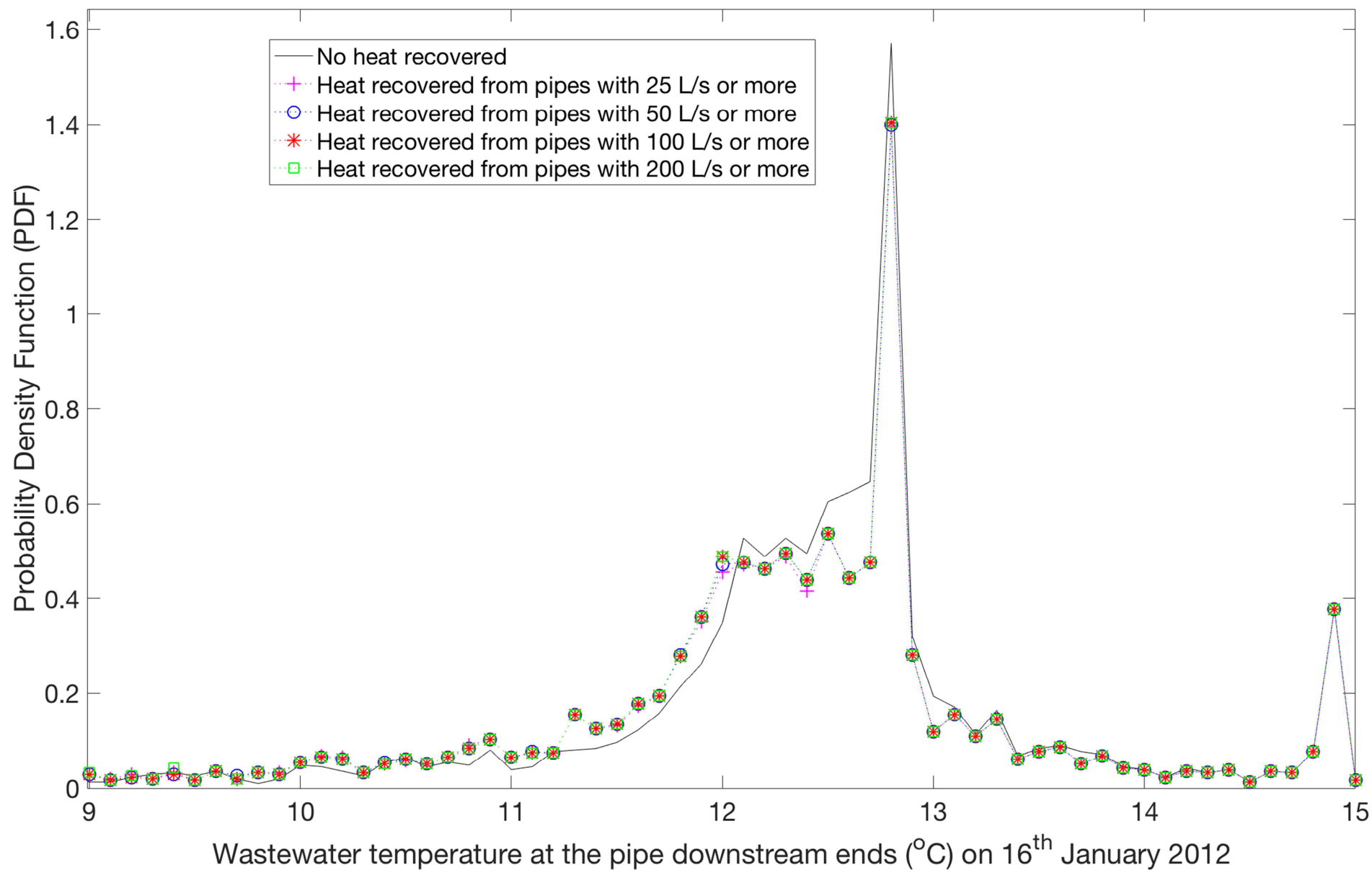


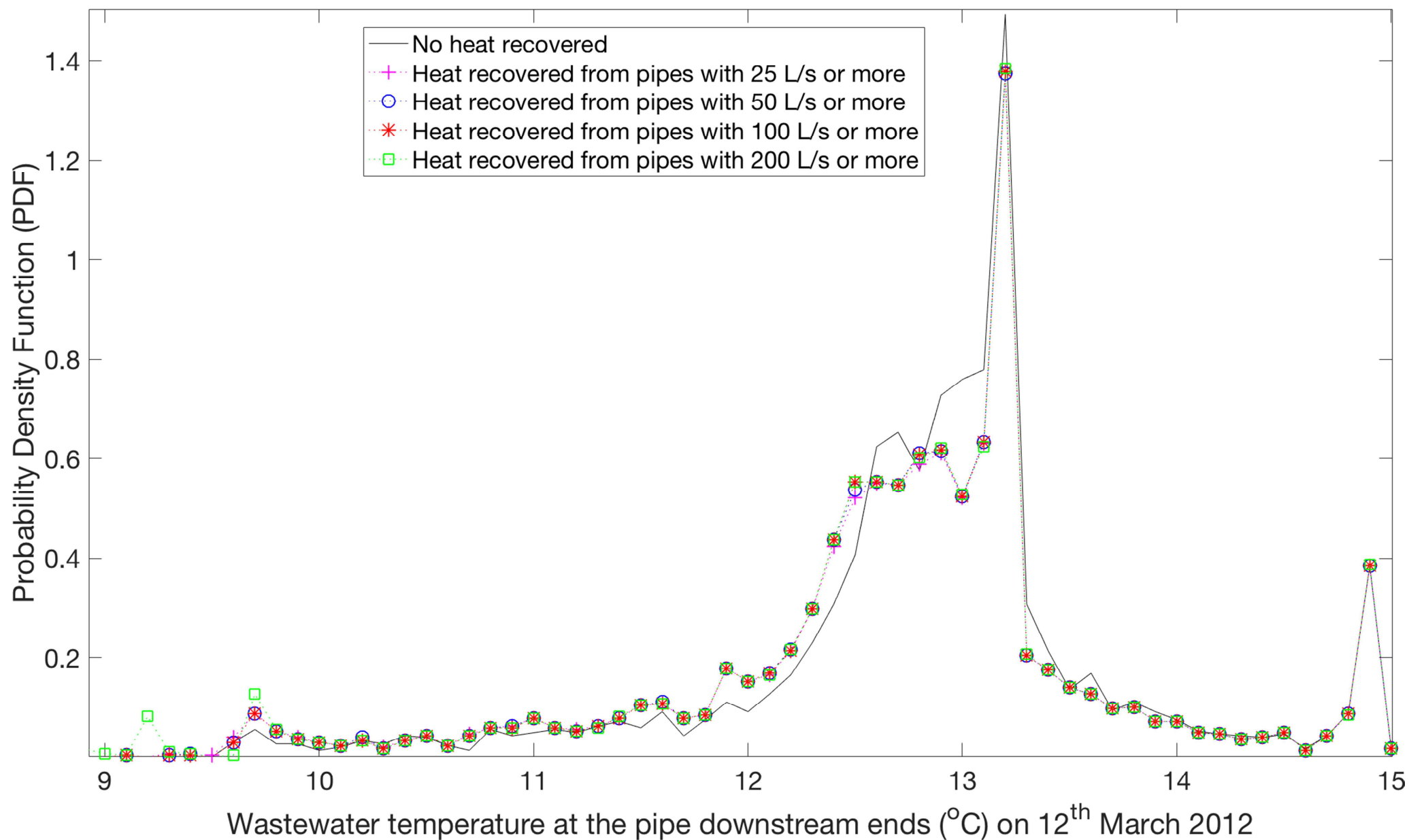
Figure 6: Probability distribution function (PDF) of the pipe downstream wastewater temperature, when heat is recovered in January, between 07:00 and 08:00 AM (Scenario 1). The PDF of temperatures below 9°C was equal/close to zero, and hence neglected in the plot.

523

524 3.5.2 Scenario 2, between 07:00 & 08:00 AM

525 Figure 7 shows the PDF of wastewater temperatures, at the downstream ends of each pipe in Scenario 2
526 between 07:00 and 08:00 AM. The heat energy recovery resulted in slightly larger probability of pipes with
527 temperatures between 11 and 12.3 °C.

ACCEPTED MANUSCRIPT



528 *Figure 7: Probability distribution function (PDF) of the pipe downstream wastewater temperature, when heat is recovered in March, between 07:00 and 08:00 AM (Scenario 2). The PDF of temperatures below 9 $^{\circ}\text{C}$ was equal/close to zero, and hence neglected in the plot.*

530 3.5.3 Scenario 3, between 07:00 & 08:00 AM

531 Figure 8 shows the PDF of pipe downstream wastewater temperatures in Scenario 3, between 07:00 and
532 08:00 AM. As expected, heat energy recovery in May results in generally higher temperatures compared to
533 Scenarios 1 and 2, and increased the probability of obtaining lower pipe temperatures (between 13.7 and
534 14.3 °C) than that of no heat recovery.

ACCEPTED MANUSCRIPT

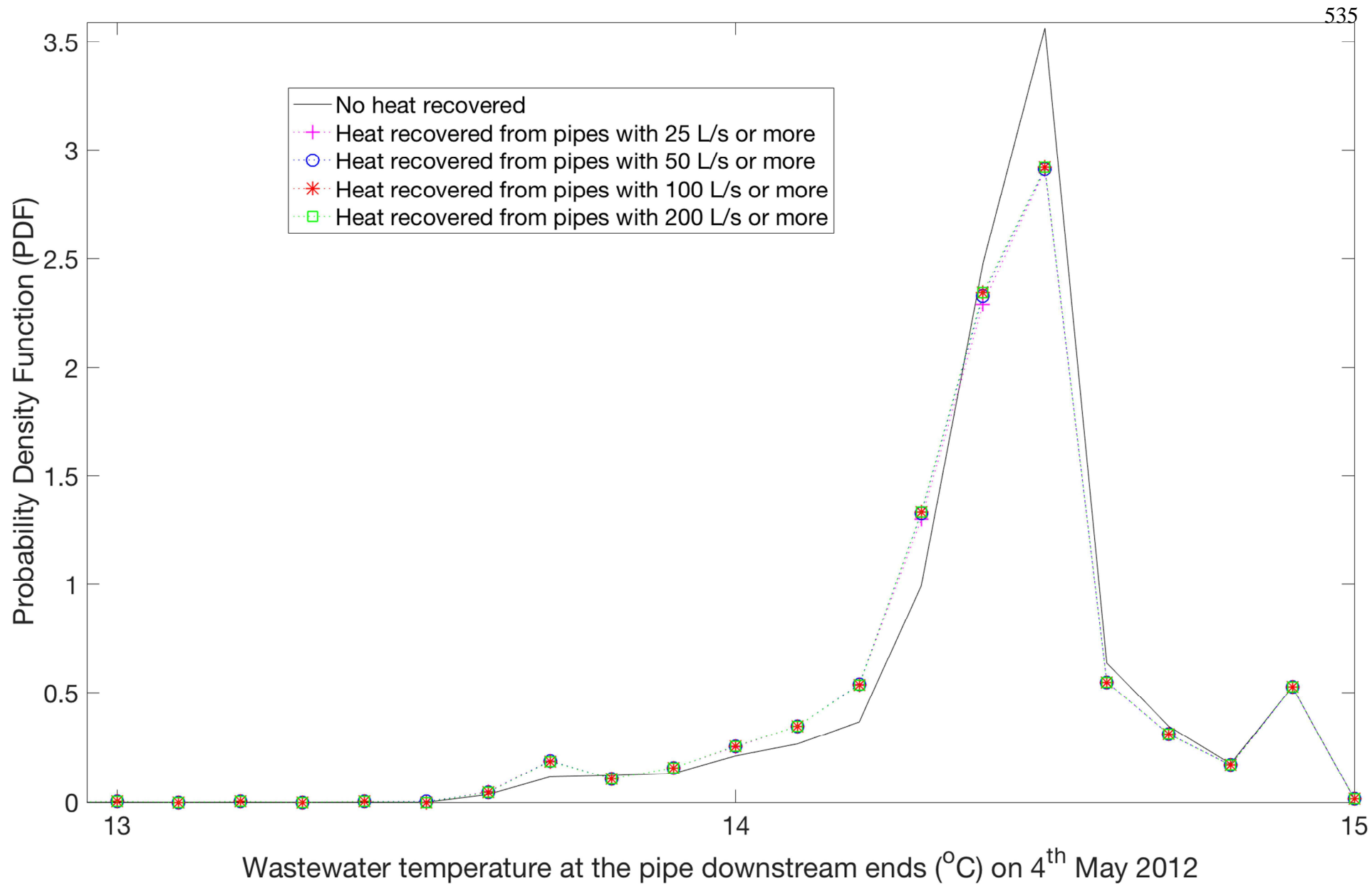


Figure 8: Probability distribution function (PDF) of the pipe downstream wastewater temperature, when heat is recovered in May, between 07:00 and 08:00 AM (Scenario 3). The PDF of temperatures below 13 $^{\circ}\text{C}$ was equal/close to zero, and hence neglected in the plot.

3.5.4 Summary of Scenarios 1, 2 & 3, between 07:00 & 08:00 AM

ACCEPTED MANUSCRIPT

Table 4 summarises the findings of Scenarios 1, 2 and 3 for the hours between 07:00 and 08:00 AM. The number of locations in Table 4 refers to the number of pipes that meet the temperature (above 9°C) and the flow (25, 50, 100 & 200 L/s or above) criteria for recovering heat (200 kW/pipe). The total heat energy recovery for each of the three scenarios was the same for each criterion, since the number of potential locations was the same. The three scenarios, presented in this section, demonstrated five potentially viable heat energy recovery options where the minimum temperatures were above the thresholds. The minimum influent temperature was around 3°C below the 9°C threshold while the temperatures in some pipes fell 2°C below the 5°C threshold.

Table 4: Summary of potential heat energy recovery results from Scenarios 1, 2 and 3 between 7:00 and 8:00 AM. HR stands for heat recovery.

Scenario	Month	Min Q	No. of HR locations, between 07:00 and 08:00 AM	Total HR between 07:00 and 08:00 AM (200kW/pipe)	WwTP Influent temperature Before HR	Minimum network temperature Before HR	WwTP Influent temperature After HR	Minimum network temperature After HR
				MWh				
1	January	25	57	11.4	12.5	8.6	7.8	7.4
		50	41	8.2				
		100	37	7.4				
		200	29	5.8				
2	March	25	57	11.4	13.0	9.7	8.2	7.8
		50	41	8.2				
		100	37	7.4				
		200	29	5.8				
3	May	25	57	11.4	14.5	13.7	9.7	9.3
		50	41	8.2				
		100	37	7.4				
		200	29	5.8				

4 Discussion

Linking a single pipe heat transfer model to a hydrodynamic model and validating the linked model in a sewer network setting enabled the investigation of potential multi-location heat energy recovery from a sewer catchment of 79500 PE. The viable potential heat energy recovery options varied depending on the month, where the lowest predicted was 116 MWh/day or 42 GWh/year, assuming a 100% efficient heat

553 recovery system. This potential viable heat energy is adequate to cover the annual heat demands of 2500,
554 3500 or 5300 households, assuming high, medium and low UK annual gas consumption of 17, 12 and 8
555 MWh/household respectively (Ofgem, 2017 and Ali et al., 2017). March and May showed potential viable
556 heat energy recovery of 58.4 and 75.7 GWh/year, that are equivalent to annual heat demands of 4900 and
557 6300 households respectively when considering the medium demand of 12 MWh/year/household.
558 Accounting for the lowest potential heat energy recovery (January) and the range of annual household
559 demand, 7 to 15% of the 79500 PE catchment annual demand can be met, without causing wastewater
560 temperatures in the network or in the WwTP influent to be below 5 and 9°C respectively, assuming 2.3 PE
561 per household. The above percentage may rise to cover 14% and 18% of the catchment heat annual demand
562 when March and May scenarios are considered respectively, assuming medium annual UK heat demand.

563
564 The rates of predicted heat recovery were presented in more details for the hours between 07:00 and 08:00
565 AM since this is considered to be the time for high heat energy demand and showed typical representation of
566 the daily DWF. Prediction results showed that setting a low flow threshold level for pipes to recover heat
567 from (e.g. 25 L/s), larger rates of heat can potentially be recovered, which consequently resulted in lower
568 wastewater temperatures (Figure 7 & Figure 8). This was expected since the lower flow rate had less
569 thermal capacity and hence caused a larger wastewater temperature reduction in sewers (Equation 1). One
570 can notice a shift in the PDF peaks from left (low temperature) in January to the higher temperatures in
571 May. This is due to the higher in-sewer air temperature (around 14.4°C) in May which was highly
572 influenced by the ambient air temperature. Table 4 showed how recovering heat of 5.8 to 8.2 MWh, in
573 Scenarios 1, 2 and 3 can be achieved while meeting the minimum temperature criteria set by the water
574 utility.

575
576 Other studies have suggested that heat recovery from wastewater may reduce the deposition of fat, oil and
577 grease (FOG) (He, et al., 2017). This is because temperature plays a major part in influencing the FOG
578 hydrolysis rate where higher temperatures increase the rate of saponification, which increases the FOG
579 deposition (Iasmin, et al., 2016). However, the latter authors performed their study on temperatures of 22

580 and 45°C, hence further research is needed to investigate the impact of temperature variation, over a more
581 typical in-sewer temperature range (e.g. 5 to 25°C), on the FOG deposit formation.

582
583 This paper has not considered the practical barriers of recovering heat from a sewer network. For example,
584 there are physical limitations on the possibility of installing heat exchangers in certain pipe sizes, which is
585 dependent on the rate of heat recovery. Future work will implement a multi criteria optimisation technique
586 to maximise the potential of heat energy recovery, within a sewer network, without compromising on the
587 wastewater treatment process, and taking into account practical issues associated with the location and
588 operation of heat exchangers.

589 **5 Conclusions**

590 A network heat transfer model, was developed and validated in this study and was implemented to assess the
591 viability of heat energy recovery scenarios, from a large Belgian sewer network serving 79500 PE. The
592 network heat transfer model was based on single pipe heat transfer model, which utilised the first principles
593 of heat transfer including the heat exchange between wastewater and in-sewer air, and was linked to a
594 hydrodynamic model to predict wastewater temperatures throughout the network over extended periods.
595 Validation of the network heat transfer model showed a daily RMSE between measured and modelled in-
596 pipe wastewater temperatures that ranged between 0.44 and 0.72 °C for the different months of the year.
597 This was based on a constant input foul temperature of 15°C, which minimised the RMSE of the measured
598 and modelled in-pipe wastewater temperatures. Three modelled seasonal scenarios showed potential heat
599 energy recovery options on an hourly basis in three days with dry weather flow during January, March and
600 May. It was found that 46% of the 288 hourly modelled heat recovery simulations predicted viable heat
601 recovery since they resulted in wastewater temperatures that were always equal or above the thresholds of 5
602 °C, in the network, and 9 °C in the WwTP influent. The predicted rate of heat energy recovery whilst
603 meeting the minimum temperature requirements varied from 116 MWh/day in January to 207 MWh/day in
604 May. This can meet 7% to 18% of the 79500 PE catchment heat demand, assuming a 100% efficient heat
605 recovery and supply system. The current network heat transfer model will be further developed to enable the
606 automated spatial optimisation of viable heat recovery locations from a large sewer network given both

607 practical constraints and the wish to achieve the highest heat recovery that satisfies local demand. Future
608 studies may also examine the temporal availability of heat and whether the rate of heat recovery can be
609 enhanced by better matching the temporal pattern of local heat demand and recovery.

610 6 References

611 Abdel-Aal, M., 2015. Modelling the Viability of Heat energy recovery from Underground Pipes-
612 Deterministic modelling of wastewater temperatures in a 3048 sewer pipes network, PhD Thesis, University
613 of Bradford. Available on <http://hdl.handle.net/10454/14467>.

614
615
616 Abdel-Aal, M., Mohamed, M., Smits, R., Abdel-Aal, R., De Gussem, K., Schellart, A. & Tait, S., 2015.
617 Predicting wastewater temperatures in sewer pipes using abductive network models. *Water Science &*
618 *Technology* 71(1), 89-96.

619
620 Abdel-Aal, M., Smits, R., Mohamed, M., De Gussem, K., Schellart, A. & Tait, S., 2014. Modelling the
621 viability of heat energy recovery from combined sewers. *Water Science & Technology*, 70, 297-306.

622
623 AECOM Building Engineering, 2014. Energy Demand Research Project: Early Smart Meter Trials, 2007-
624 2010. [data collection]. UK Data Service. SN: 7591, <http://doi.org/10.5255/UKDA-SN-7591-1>

625
626 Ali A., Mohamed, M., Abdel-Aal, M., Schellart, A. & Tait, S., 2017. Analysis of ground source heat pumps
627 performance installed in residential houses in the north of England. *Proceedings of the Institution of Civil*
628 *Engineers*, 170, 103-115.

629
630 Aquafin, 2014. Hydronaut procedure 6.5 versie Juni 2014 (In Dutch, Specifications for monitoring
631 campaigns and model validation: Internal report by Aquafin). Aartselaar: Aquafin.

632
633 Aquafin, 2015. Final report on Innovative energy recovery strategies in the urban water cycle, 2015.
634 Available on <http://inners.eu/wp-content/uploads/2015/07/Final-report-INNERS-project.pdf> [Accessed 05
635 October 2017].

636
637 Bischofsberger, W., Seyfried, C.F. 1984. Wärmeentnahme aus Abwasser (Heat Extraction from
638 Wastewater), Lehrstuhl und Prüfamnt für Wassergütwirtschaft und Gesundheitsingenieurwesen der
639 Technischen Universität München, Garching.

640
641 Buri, B., & Kobel, R. 2005. Energie Aus Kanalabwasser Leitfaden für Ingenieure und Planer (Channel
642 Waste Energy- Guidance for engineers and planners). Available on [http://www.ib-](http://www.ib-salzmann.de/energie_aus_abwasser/leitfaden_fuer_ingenieure_planer.pdf)
643 [salzmann.de/energie_aus_abwasser/leitfaden_fuer_ingenieure_planer.pdf](http://www.ib-salzmann.de/energie_aus_abwasser/leitfaden_fuer_ingenieure_planer.pdf) [Accessed 29 May 2018].

644
645
646 Cipolla, S. & Maglionico, M., 2014. Heat energy recovery from urban wastewater: Analysis of the
647 variability of flow rate and temperature. *Energy and Buildings* 69, 122-130.

648
649 Defra- Department for Environment, Food and Rural Affairs, 2002. Sewage Treatment in the UK- UK
650 Implementation of the EC Urban Waste Water Treatment Directive.

651
652 Dürrenmatt, D.J., 2006. Berechnung des Verlaufs der Abwassertemperatur im Kanalisationsrohr
653 (Calculation of wastewater temperature profiles in sewers), Master's thesis, Swiss Federal Institute of
654 Technology (ETH), Zurich, Switzerland.

656 Dürrenmatt, D.J. & Wanner, O., 2008. Simulation of the wastewater temperature in sewers with TEMPEST.
657 Water Science & Technology 57 (11), 1809-1815. D MANUSCRIPT

659 Dürrenmatt, D.J., & Wanner, O., 2014. A mathematical model to predict the effect of heat recovery on the
660 wastewater temperature in sewers. Water Research 48(1), 548-558.

662 DWA- Deutsche Vereinigung für Wasserwirtschaft, Abwasser und Abfall e.V. 2009. Energie aus Abwasser
663 - Wärme- und Lageenergie. (Energy from wastewater- heat and potential energy DWA-Regelwerk,
664 Merkblatt DWA-M 114, Hennef.

666 ECUK, Energy Consumption in the UK, 2017. Department for Business, Energy & Industrial Strategy.
667 Available on <https://www.gov.uk/government/statistics/energy-consumption-in-the-uk> [Accessed 25 January
668 2018].

670 Edwini-Bonsu, S. & Steffler, P. M., 2006. Modeling Ventilation Phenomenon in Sanitary Sewer Systems: A
671 System Theoretic Approach, Journal of Hydraulic Engineering, 132, 778–790.

673 Elías-Maxil., J.A. 2015. Heat modeling of wastewater in sewer networks- Determination of thermal energy
674 content from sewage with modeling tools, PhD Thesis, TU Delft.

676 Elías-Maxil, J.A., Hofman, J., Wols, B., Clemens, F., van der Hoek, J.P. & Rietveld, L., 2017. Development
677 and performance of a parsimonious model to estimate temperature in sewer networks. Urban Water Journal,
678 14 (8), 829-838.

680 Flinspach, D., 1973. Wärmelastplan neckar plochingen bis mannheim stand. Ministerium für Ernährung,
681 Stuttgart.

683 He, X., Reyes, F. L. & Ducoste, J. J., 2017. A critical review of fat, oil, and grease (FOG) in sewer
684 collection systems: Challenges and control', Critical Reviews in Environmental Science and Technology, 47
685 (13), 1191–1217.

687 Iasmin, M., Dean, L. O. & Ducoste, J. J., 2016. Quantifying fat, oil, and grease deposit formation kinetics,
688 Water Research, 88, 786–795.

690 Kretschmer, F., Weissenbacher, N., Ertl. T., 2015. Integration of Wastewater Treatment Plants into Regional
691 Energy Supply Concepts. Sustainable Sanitation Practice, 22, 4-9.

693 Kretschmer, F., Simperler L. & Ertl., T., 2016. Analysing wastewater temperature development in a sewer
694 system as a basis for the evaluation of wastewater heat recovery potentials. Energy and Buildings, 128, 639-
695 648.

697 Metcalf & Eddy, 2004. Wastewater engineering treatment and reuse. 4th edition, New York: Mcgrow Hill.

699 Ofgem- Office of Gas and Electricity Markets, 2017. Typical Domestic Consumption Values. Available on
700 [https://www.ofgem.gov.uk/gas/retail-market/monitoring-data-and-statistics/typical-domestic-consumption-](https://www.ofgem.gov.uk/gas/retail-market/monitoring-data-and-statistics/typical-domestic-consumption-values)
701 [values](https://www.ofgem.gov.uk/gas/retail-market/monitoring-data-and-statistics/typical-domestic-consumption-values) [Accessed 29 August 2017].

703 Schilperoort, R.P. & Clemens, F.H., 2009. Fibre-optic distributed temperature sensing in combined sewer
704 systems. Water Science & Technology 60 (5), 1127-1134.

706 Shammass, N.K., 1986., Interactions of temperature, ph and biomass on the nitrification process. Water
707 Pollution Control Federation, 58, 52-59.

709 Simperler, L., 2015. Impact of thermal use of wastewater in a sewer on the inlet temperature of a wastewater
710 treatment plant, Master's Thesis, University of Natural Resources and Life Sciences.

711
712 Sitzenfrei, R., Hillebrand S., & Rauch W., 2017. Investigating the interactions of decentralized and
713 centralized wastewater heat recovery systems. *Water Science and Technology*, 75, 1243-1250.

714
715 Vlario, 2015. Heat energy recovery from the sewer system. Available on
716 [http://www.vlario.be/site/files/Appendix-6-Heat-recovery from-the-sewer-system.pdf](http://www.vlario.be/site/files/Appendix-6-Heat-recovery%20from-the-sewer-system.pdf) [Accessed 19
717 October 2017].

718
719 Wanner, O., Panagiotidis, V., Clavadetscher, P. & Siegrist, H., 2005. Effect of heat recovery from raw
720 wastewater on nitrification and nitrogen removal in activated sludge plants. *Water Research*, 39, 4725-4734.

ACCEPTED MANUSCRIPT

- Potential of heat recovery from a large sewer network was modelled for the first time
- Linked network heat transfer and network hydrodynamic models were validated
- Scales of potential viable heat recovery varied seasonally from 116 to 207 MWh/day
- Viable heat recovery can meet 7% to 18% of a 79500 PE catchment demands

ACCEPTED MANUSCRIPT